

*Letter to the Editor***Vertical mass flux in a sunspot penumbra****R. Schlichenmaier and W. Schmidt**

Kiepenheuer-Institut für Sonnenphysik, Schöneckstrasse 6, D-79104 Freiburg, Germany (schliche,wolfgang@kis.uni-freiburg.de)

Received 26 July 1999 / Accepted 12 August 1999

**Abstract.** We present the first direct measurement of vertical motion in the deepest atmospheric layers of a penumbra, obtained at hitherto unreached spatial resolution. Isolated hot upflows in the inner penumbra feed the horizontal Evershed flow that is observed in the mid and outer penumbra. We discover cool downflows which surround the hot upflows in the inner penumbra. At the outer edge of the penumbra, the Evershed flow terminates in a ring of downflow channels. The upflows transport a sufficient amount of energy to account for the observed brightness of the penumbra. These measurements have therefore significant implications for understanding the mass balance and the energy transport in a sunspot penumbra.

**Key words:** Sun: photosphere – Sun: sunspots – Sun: magnetic fields

**1. Introduction**

Sunspots are ideally suited to study plasma motion in the presence of a strong magnetic field. While the gas in the cool umbra of a sunspot is at rest, vigorous mass flows on small spatial scales are present in the penumbra. The most prominent penumbral velocity pattern is a horizontal outflow, known as the Evershed flow (Evershed 1909).

The Evershed flow is characterized by strong wavelength shifts and line asymmetries of photospheric absorption lines, which depend on the location in the penumbra, the viewing angle, and the strength of the line (Stellmacher & Wiehr 1980; Ichimoto 1987). Observations of spectral lines with various heights of origin indicate that the Evershed flow is concentrated in elevated channels (Rimmele 1995a; Stanchfield et al. 1997), which are too thin to be resolved by any existing solar telescope. The line asymmetry is then interpreted in terms of horizontal inhomogeneities (Wiehr 1994) and flow channels which are thinner than the layer in which the line is formed (Solanki & Montavon 1993; Degenhardt 1993; Schlichenmaier et al. 1998).

**2. Observations**

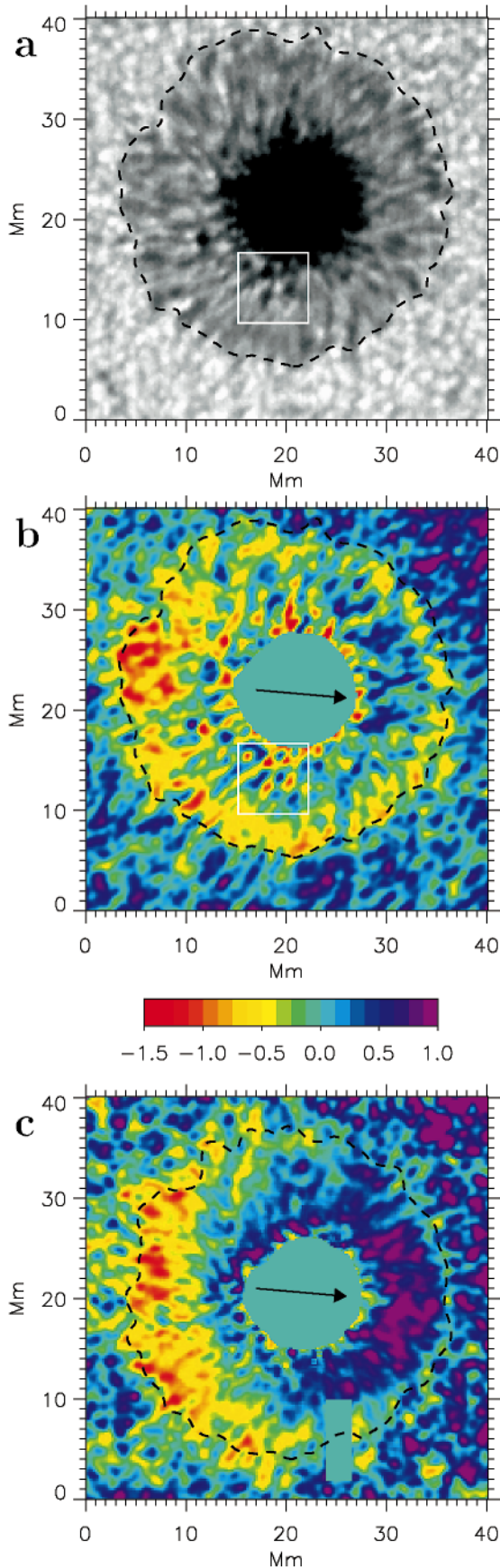
We have measured material flows at different heights in the photosphere of a fairly large round sunspot (NOAA 8578, 9 Nov 1998), observed near disk centre at a position angle of  $\theta = 12^\circ$ . The spatial resolution of the data is about 0.5 arcsec, corresponding to 350 km on the Sun. Two-dimensional spectra of the whole sunspot and its immediate surroundings were taken in the weak C I line at 538.0 nm, which forms in the deepest photospheric layers, and in the Fe II 542.5 nm line, a rather temperature-sensitive line which forms in the mid-photosphere at a height of about 100 km above the continuum level. Both lines are well-suited to observe flows in the lower penumbral photosphere.

The observations have been made with the Vacuum Tower Telescope of the Kiepenheuer-Institut, operated at the Observatorio del Teide on Tenerife, using the Telecentric Solar Spectrometer (TESOS) (Kentischer et al. 1998), which is based on two Fabry-Perot interferometers. This instrument permits velocity measurements with a precision of about  $100 \text{ m s}^{-1}$ . Each data set (“spectrum”) consists of a series of narrowband images with a bandwidth of 2 pm, taken at 20 wavelength positions equally spaced across the spectral line, and of simultaneously taken broadband continuum images with the same field of view.

Fig. 1a shows a continuum image representing an area of  $40 \times 40 \text{ Mm}^2$ . The dashed black line at 88% of the mean solar intensity marks the outer boundary of the penumbra. The individual narrowband images of each spectrum were carefully aligned with respect to each other, in order to remove residual image motion. Image distortion caused by the earth atmosphere was removed by a destretching algorithm (Rimmele 1994).

**3. Results**

Line shifts were measured using a Fourier transform method (Schmidt et al. 1999): the phase of the first Fourier component of the line profile provides the wavelength position of the line. This method is very insensitive to noise and, therefore, especially suited for weak lines. Line shifts were converted into velocities using the Doppler formula. The velocity origin was defined by setting the average velocity of the granulation in the vicinity of the sunspot to a value of  $+0.4 \text{ km s}^{-1}$ , to account for the convective blueshift (Balthasar 1988). In the umbra, at



intensities below 30% of the mean solar intensity, the lines are too weak to determine velocities, and the corresponding values have been set to zero. Fig. 1b shows the flow map of the deep photosphere derived from the spectrum of the carbon line. The field of view is identical to Fig. 1a. The velocity range is from  $-1.5 \text{ km s}^{-1}$  to  $+1 \text{ km s}^{-1}$ , where negative (positive) values denote flows away from (towards) the observer. Fig. 1c is the flow map of the mid-photospheric layers of the same spot, measured in the iron line, about one hour later. The colour coding is the same as in Fig. 1b. A small area in the lower part of Fig. 1c contains no data due to an imperfection of the interference filter used for this measurement.

Doppler velocities derived from line shifts are always line-of-sight velocities. We make use of the approximate azimuthal symmetry of the observed sunspot and its penumbral flow pattern, in order to distinguish between the horizontal and the vertical part of the measured flow. The line-of-sight component of a horizontal velocity changes sign around the circumference of the spot, because it is proportional to  $\sin \theta \cdot \cos \phi$ , where  $\phi$  is the azimuth angle around spot centre, with  $\phi = 0$  pointing to the centre of the disk. The constant angle  $\theta$  is measured between the line of sight and the normal to the spot surface. The vertical component is proportional to  $\cos \theta$  and thus independent of the azimuth angle. In the deepest layers we find a ring of small areas of blueshift in the inner part of the penumbra (see Fig. 1b). This pattern is independent of the azimuth position and therefore corresponds to vertical motion. The blueshifts are also visible higher up in the photosphere (see Fig. 1c). Earlier observations have found isolated patches of blueshift in near-disk centre sunspots (Rimmele 1995a; Stanchfield et al. 1997; Westendorp et al. 1997), but those measurements did not permit to determine the flow direction, since they have only been taken on the disk centre side of the penumbra.

Interlaced with the upflow channels in the inner penumbra, we find a pattern of concentrated downflows. They are conspicuous in the deepest layers (see Fig. 1b) and are almost absent in the mid-photosphere (see Fig. 1c). The subfield shown in Fig. 2 demonstrates the close correspondence between intensity and the orientation of the velocity field. Upflows are always found in bright regions, known as “penumbral grains”, while downflows occur in dark areas. Thus, upflows are hot while downflows are cool.

**Fig. 1a–c.** Sunspot near the centre of the solar disk at a position angle of  $12^\circ$ . The displayed area corresponds to  $40 \times 40 \text{ Mm}^2$  on the Sun. **a**, Broadband continuum image. The broken black line marks the outer boundary of the penumbra. The small square indicates the subfield shown in Fig. 2a. **b**, Velocity field of the deepest photospheric layers, derived from shifts of the carbon line at  $538.0 \text{ nm}$ . Positive velocities point out of the Sun and correspond to a upflow. The colour coding ranges from  $-1.5 \text{ km s}^{-1}$  (red, downflow) to  $+1.0 \text{ km s}^{-1}$  (blue, upflow). The black line is identical to Fig. 1a. The arrow points toward the centre of the solar disk. The small square indicates the subfield shown in Fig. 2b. **c**, Velocity of the mid-photospheric layer, derived from the ionized iron line at  $542.5 \text{ nm}$ . The same color coding is used as in 1b.

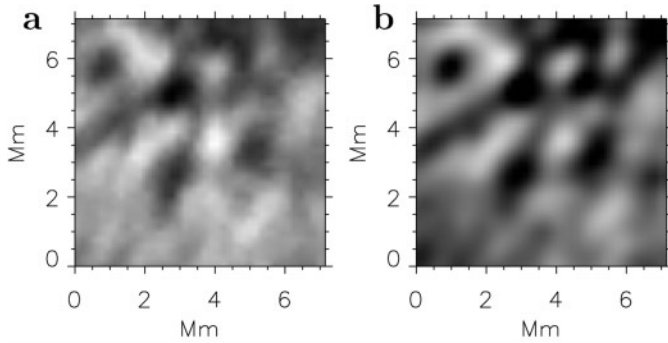


**Fig. 2a and b.** Subfield of  $7 \times 7 \text{ Mm}^2$  of Figs. 1a and b. **a**, Continuum image. **b**, Velocity field. The greyscale of Fig. 2b ranges from  $-1 \text{ km s}^{-1}$  (black) to  $+1 \text{ km s}^{-1}$  (white). The images are highly correlated, i.e., bright material moves upwards and vice versa.

The velocity pattern of the mid-layers shows a strong azimuthal variation in the central and outer penumbra (see Fig. 1c), more pronounced than in the deep photosphere, indicating the presence of the “classical” Evershed flow. It is well known that the flow is nearly horizontal in this part of the penumbra (Schröter 1965; Title et al. 1993). Since our observations are made at  $\theta = 12^\circ$ , the line-of-sight velocities with a magnitude of  $\pm 1 \text{ km s}^{-1}$  correspond to a horizontal flow speed of  $\pm 5 \text{ km s}^{-1}$ .

The continuation of the mass flux at the outer penumbral boundary (Rimmele 1995a, 1995b; Solanki et al. 1994) is a long-debated issue. There is observational evidence that a few tenths of the mass flux extends beyond the outer penumbral boundary and rises up into the superpenumbral magnetic canopy that surrounds a sunspot some 300 km above the photosphere (Solanki et al. 1992, 1994, 1999). From an inversion of polarimetric measurements, Westendorp et al. (1997) recently inferred downflows immediately outside the penumbra. Our *direct* measurements confirm these downflows at much higher spatial resolution, but we find that they are located mainly at or *inside* the outer penumbral boundary. Fig. 1b shows the observed chain of downflows with speeds between  $-0.5$  and  $-1.0 \text{ km s}^{-1}$ . In higher layers, the downflows are less pronounced, but still visible.

#### 4. Discussion

Two models for the Evershed flow are presently discussed. In both cases, the flow is channeled along a magnetic flux tube and is accelerated by a gas pressure gradient. The “siphon flow” model (Meyer & Schmidt 1968; Degenhardt 1991; Montesinos & Thomas 1997) is based on a magnetic flux tube that arches from inside the penumbra to or beyond the outer penumbral boundary. Here the gas pressure gradient is caused by differing magnetic field strengths at the footpoints of the arch. The second model is based on a numerical simulation of a moving thin magnetic flux tube embedded in a magnetostatic sunspot (Schlichenmaier et al. 1998). It describes the evolution of a tube that initially lies along the boundary between the penumbra and the non-magnetic surrounding Sun. Initiated by a radiative in-

stability, the tube rises through the deep, convectively unstable penumbra. During the rise, the flow along the tube develops. In this “moving tube” model the gas pressure gradient is caused by the convectively unstable stratification beneath the photosphere and is sustained by a decreasing gas pressure as the hot upflow cools by radiative losses in the photosphere.

Our observation clearly demonstrates the existence of vertical upflows in the inner penumbra, which are compatible with both models. In accordance with other observations we measure a horizontal flow from the inner to the outer penumbra, which for our spot amounts to a distance of about 8 000 km. A major shortcoming of the siphon flow loops (Montesinos & Thomas 1997) is the rather short footpoint separation of 1 500 km at most. Longer loops are possible, but they lead to unrealistic heights for the top of the arch. In the moving tube model, the tube bends horizontally at its footpoint and continues to the outer penumbral boundary with an elevation of only some 100 km above continuum optical depth unity. This is consistent with our observations. However, the downflows that we observe at the outer penumbral boundary are not described by that model. Siphon flows by definition have a downstream at the outer footpoint and they can in principle explain the observed downflow at or beyond the outer penumbral boundary (Montesinos & Thomas 1997), although the observed distance between up- and downflows is incompatible with the computed loop lengths.

The moving tube model predicts upflow channels which enter the photosphere at a temperature of 12 000 K. The flow cools to 5 000 K by radiative heat loss and a single tube deposits an amount of  $3 \cdot 10^8 \text{ J kg}^{-1}$  of thermal energy at a density of  $2 \cdot 10^{-4} \text{ kg m}^{-3}$  in the penumbra (cf., Schlichenmaier et al. 1999). With the highest measured upflow velocity of  $1 \text{ km s}^{-1}$  we estimate a heat flux of  $6 \cdot 10^7 \text{ W m}^{-2}$  that emerges from our brightest feature. This value is close to the solar constant (Stix 1991) of  $6.3 \cdot 10^7 \text{ W m}^{-2}$  and is consistent with the observational finding that the brightest penumbral grains are about as bright as the quiet sun (Collados et al. 1988; Denker 1998). We conclude that the observed upflows near the inner boundary of the penumbra can, in principle, explain the surplus brightness of the penumbra as compared to the umbra.

Further measurements of the velocity and the magnetic field configuration, with a resolution of 100 km on the Sun and a time coverage of a few hours, are needed to obtain a consistent description and a physical model of the small scale dynamics of the sunspot penumbra.

*Acknowledgements.* We are grateful to M. Schüssler for valuable comments on the manuscript. Part of this work was supported by the *Deutsche Forschungsgemeinschaft, DFG*.

#### References

- Balthasar H., 1988, *A&AS* 72, 473
- Collados M., del Toro Iniesta J.C., Vázquez M., 1988, *A&A* 195, 315
- Degenhardt D., 1991, *A&A* 248, 637
- Degenhardt D., 1993, *A&A* 277, 235
- Denker C., 1998, *Solar Phys.* 180, 81
- Evershed J., 1909, *MNRAS* 69, 454

- Ichimoto K., 1987, PASJ 39, 329
- Kentischer T., Schmidt W., Sigwarth M., v. Uexküll M., 1998, A&A 340, 569
- Meyer F., Schmidt, H.U., 1968, Zeitschr. für angew. Mathem. und Mech. 48, T219
- Montesinos B., Thomas J.H., 1997, Nat 390, 485
- Rimmele T., 1994, A&A 290, 972
- Rimmele T., 1995a, A&A 298, 260
- Rimmele T., 1995b, ApJ 445, 511
- Schlichenmaier R., Jahn K., Schmidt H.U., 1998, A&A 337, 897
- Schlichenmaier R., Bruls J.H.M.J., Schüssler M., 1999, A&A in press
- Schmidt W., Stix M., Wöhl H., 1999, A&A 346, 633
- Schröter E.H., 1965, Zeitschrift f. Astrophysik 62, 228
- Solanki S.K., Montavon C.A.P., 1993, A&A 275, 283
- Solanki S.K., Rüedi I., Livingston W., 1992, A&A 263, 339
- Solanki S.K., Montavon C.A.P., Livingston W., 1994, A&A 283, 221
- Solanki S.K., Finsterle W., Rüedi I., Livingston W., 1999, A&A 347, L27
- Stanchfield II D.C.H., Thomas J.H., Lites B.W., 1997, ApJ 447, 485
- Stellmacher G., Wiehr E., 1980, A&A 82, 157
- Stix M., 1991, The Sun, Springer Verlag, Berlin, Heidelberg
- Title A.M., Frank Z.A., Shine R.A., et al., 1993, ApJ 403, 780
- Westendorp Plaza C., del Toro Iniesta J.C., Ruiz Cobo B., et al., 1997, Nat 389, 47
- Wiehr E., 1994, A&A 298, L17